PAPER

Check for updates

Structure transition of a C_{60} monolayer on the Bi(111) surface

Ya-Ru Wang, Min-Long Tao, [ID] * Ma Chao-Ke, Zi-Long Wang, Da-Xiao Yang, Ming-Xia Shi, Kai Sun, Ji-Yong Yang and Jun-Zhong Wang [ID] *

The interfacial structures of C_{60} molecules adsorbed on solid surfaces are essential for a wide range of scientific and technological processes in carbon-based nanodevices. Here, we report structural transitions of the C_{60} monolayer on the Bi(111) surface studied *via* low-temperature scanning tunneling microscopy (STM). With an increase in temperature, the structure of the C_{60} monolayer transforms from local-order structures to a ($\sqrt{93} \times \sqrt{93}$) R20° superstructure, and then to a (11 × 11) R0° superstructure. Moreover, the individual C_{60} molecules in different superstructures have different orientations. C_{60} molecules adopt the 6 : 6 C–C bond and 5 : 6 C–C bond facing-up, mixed orientations, and hexagon facing-up in the local-order structure, ($\sqrt{93} \times \sqrt{93}$) R20°, and (11 × 11) R0° superstructure, respectively. These results shed important light on the growth mechanism of C_{60} molecules on solid surfaces.

Introduction

C_{60} molecule, as a prototypical fullerene molecule, has attracted widespread attention due to its potential in endohedral fullerenes,[1] photovoltaic devices,[2] peapod nanotubes,[3] and single-molecule transistors.[4] A C_{60} monolayer grown on solid surfaces is critical for understanding and controlling the interfacial properties of fullerene-derived electronic and photovoltaic devices.[5,6] STM studies demonstrated that the C_{60} monolayer on the solid surface exhibit a variety of lattice orientations such as the "in phase" ($2\sqrt{3} \times 2\sqrt{3}$) R30°,[7–13] (7 × 7) R0°[13] and ($\sqrt{589} \times \sqrt{589}$) R14.5°.[13–15] The individual molecules of fullerene and fulleride within a single domain display different orientations. In the complex orientational ordering (7 × 7) R0° structure, a 7-molecule C_{60} cluster consists of a central molecule sitting atop of a gold atom and six tilted surrounding molecules.[10] In the unit cell of the ($\sqrt{589} \times \sqrt{589}$) R14.5° structure, 49 C_{60} molecules adopt 11 different orientations.[14] In the ($2\sqrt{3} \times 2\sqrt{3}$) R30° structure, all C_{60} molecules are in the same orientation.[12,16] The complex chiral motifs have been observed.[17] In $CsnC_{60}$ fulleride films, orientational ordering appears.[18] Moreover, "bright" and "dim" molecules have been widely found in the C_{60} monolayer.[9–17] However, the "dim" molecules in superstructures reported so far arrange irregularly.

The structure of C_{60} monolayers grown on the solid surface is not only related to C_{60} molecules themselves but also the substrate. In the past reports, there have been a large number of investigation on the C_{60} monolayer structures grown on numerous metals or semiconducting substrates, such as

Ag,[7–9,19,20] Au,[10–16,21,22] Cu,[23–25] graphene,[26,27] Si,[28,29] Ge,[30] C_{60},[29] or NaCl.[31] However, few reports address the superstructure of C_{60} molecules adsorbed on semi-metal substrates. It is found that thin films of organic molecules grown on a semi-metallic Bi(111) surface shows a lot of interesting phenomena, such as the ordered crystalline layer with the standing-up orientation of pentacene molecules,[32] the chiral self-assembly of rubrene molecules,[33] structural transitions in different monolayers of cobalt phthalocyanine films,[34] and the Moire' pattern in C_{60} thin films.[35]

In this study, we use Bi(111) as the substrate and studied the structure transition of the C_{60} monolayer. C_{60} molecules were deposited at 100 K form local-order structures. When the deposition temperature increased to room temperature, the local-order structures turn into a long-range ordered ($\sqrt{93} \times \sqrt{93}$) R20° superstructure. After annealing at 400 K, the ordered superstructure transforms into the (11 × 11) R0° superstructure. These superstructures are different from the structures of the C_{60} monolayer reported so far. Furthermore, the individual C_{60} molecules in the local-order structure, ($\sqrt{93} \times \sqrt{93}$) R20° and (11 × 11) R0° superstructure, show the 6 : 6 C–C bond and 5 : 6 C–C bond facing-up, mixed orientations, and hexagon facing-up, respectively. The 6 : 6 (5 : 6) C–C bond indicates the common side of two adjacent hexagons (pentagon and hexagon) in C_{60} molecules.

Experimental

The experiments were conducted in an ultra-high vacuum low-temperature scanning tunneling microscope produced by Unisoku. The base pressure was kept at ~1.2 × 10^{-10} Torr. An Si(111) substrate was continuously degassed at ~870 K for 8 h

School of Physical Science and Technology, Southwest University, Chongqing, China. E-mail: taotaole@swu.edu.cn; jzwangcn@swu.edu.cn

Paper

with subsequent flashing to 1400 K for several seconds. The Bi(111) film was prepared by depositing 20 monolayers of bismuth atoms on a Si(111)-7 × 7 surface at room temperature with subsequent annealing at 400 K.[36] C_{60} molecules were deposited onto the Bi(111) surface by heating the tantalum cell to 700 K. The growth rate of C_{60} molecules was about 0.4 monolayers per minute. All STM images were acquired with a tungsten tip in constant-current mode at liquid nitrogen temperature (78 K).

Results and discussion

First, a small number of C_{60} molecules were deposited onto the Bi(111) surface when the substrate was maintained at 100 K. Fig. 1(a) shows the atomic-resolution image of the hexagonal lattices of the Bi(111) thin film. The lattice constants of the Bi(111) surface are measured to be $a_1 = a_2 = 0.45 \pm 0.02$ nm, very close to the bulk value ($a = 0.454$ nm) in Bi crystals.[36] Fig. 1(b) shows the isolated C_{60} molecules on the Bi(111) surface presenting round protrusions. When reducing the bias voltage, the round protrusions are separated into two asymmetrical [Fig. 1(c)] or symmetrical [Fig. 1(d)] lobes, corresponding to the two different adsorption configurations, 5 : 6 C–C bond facing-up and 6 : 6 C–C bond facing-up, similar to C_{60} molecules on Au(111).[12] This indicates that there are two stable adsorption orientations of isolated C_{60} molecules on the Bi(111) substrate, 6 : 6 C–C bond, and 5 : 6 C–C bond facing-up.

When the coverage increases, C_{60} molecules form the close-packed hexagonal structure, as shown in Fig. 2. We noticed that all the C_{60} molecules present a uniform height, except a few dim molecules (marked by green dotted circles). The brightness contrast in images stems from the different adsorption sites of C_{60} molecules. It is well known that metal surfaces do not behave as rigid templates for the chemisorption of C_{60} molecules, but may reconstruct substantially to accommodate the molecules.[37] We speculate that Dim C_{60} molecules are located at

the vacancies of the Bi(111) substrate, originating from the reconstruction of the Bi(111) surface, similar to C_{60} molecules on Au(111)[16] and Cu(111).[38]

According to the arrangement of bright and dim molecules, we can see some local-order structures, though there is a lack of long-range ordering. In Fig. 2(a), there is an (11 × 8) R0° local-order structure (marked by red parallelogram). The lattice directions of (11 × 8) R0° are along with the directions of Bi(111), and the measured lattice constants are 5.00 ± 0.02 nm and 3.64 ± 0.02 nm, corresponding to 11 and 8 times of the lattice constant of the Bi(111) surface. The lattice directions of Bi(111) were obtained on the surface, which was not covered with C_{60} molecules. In another domain, shown in Fig. 2(b), the local-order structure is mixed with three types of structures, namely (11 × 8) R0° (red quadrilateral), (11 × 11) R0° (white quadrilateral), and (10 × 8) R10° (blue quadrilateral). In particular, we noticed that C_{60} molecules exhibit almost the same orientation in a single domain, and most of the individual C_{60} molecules in the local-order structure adopt two favorite orientations (6 : 6 C–C bond and 5 : 6 C–C bond facing up) as the isolated molecules on Bi(111). For example, most of the molecules shown in Fig. 2(a) present two symmetrical lobes, corresponding to C_{60} molecules with a 6 : 6 C–C bond facing up. However, in Fig. 2(b), the molecules present two asymmetric lobes, corresponding to the 5 : 6 C–C bond facing up. We suggest that the formation of a local-order structure is due to the low-temperature growth. Because of the low kinetic energy of C_{60} molecules at 100 K, molecular mobility is not high enough to form a long-range ordered superstructure. The C_{60} molecules adsorbed on Bi(111) adopt their preferred orientations (6 : 6 C–C bond and 5 : 6 C–C bond facing up), similar to the isolated molecules adsorbed on the substrate. This proves the strong molecule–substrate interaction in the local-order structure.

To investigate the influence of temperature on the structure, we deposited C_{60} molecules on Bi(111) at room temperature. It
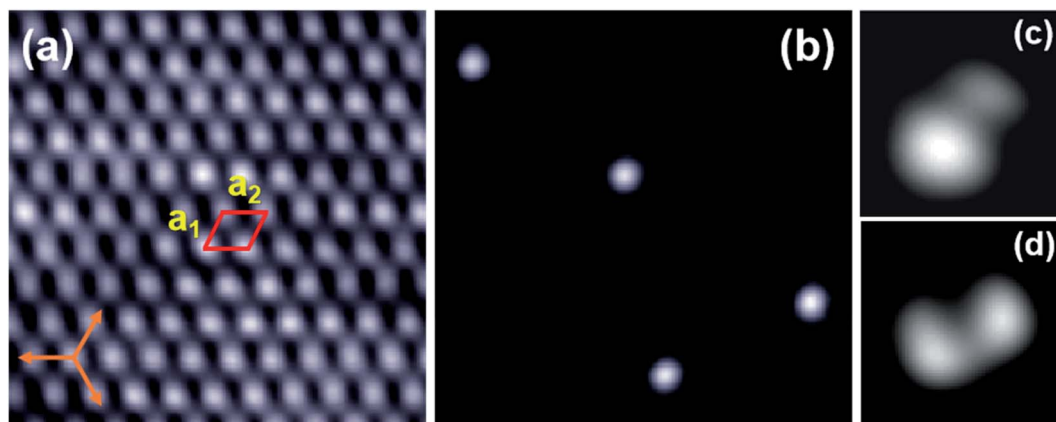

Fig. 1 The initial stage of C_{60} molecules adsorbed on the Bi(111) surface. (a) Hexagonal lattices of the Bi(111) surface, 5 nm × 5 nm, −0.1 V. The unit cell is marked with a red box and the orange arrows indicate the directions of the Si(111) substrate. (b) Isolated C_{60} molecules adsorbed on Bi(111), 20 nm × 20 nm, 2.2 V. (c) STM image of an isolated C_{60} molecule with two asymmetrical lobes corresponding to the 5 : 6 C−C bond facing up, 1.3 nm × 1.3 nm, 400 mV. (d) STM image of an isolated C_{60} molecule with two symmetrical lobes corresponding to the 6 : 6 C−C bond facing up, 1.3 nm × 1.3 nm, 200 mV.
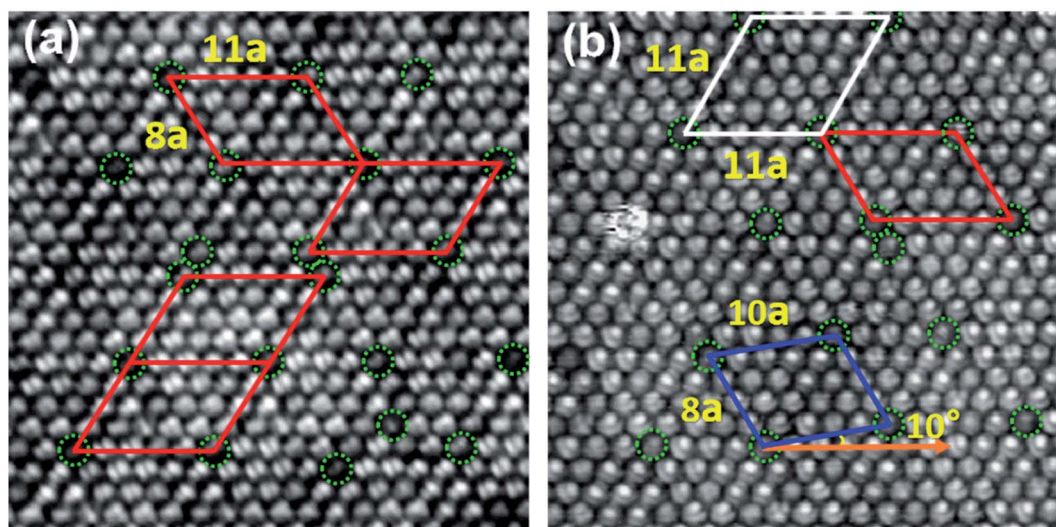
Fig. 2 Local-order structure in the monolayer C_{60} grown at a low temperature ($\sim$100 K). (a) Four unit cells of the (11 × 8) R0° superstructure appeared in the C_{60} monolayer, 20 nm × 20 nm, −1.2 V. The dim C_{60} molecules, located at the hollow position of Bi(111), are marked by the green dotted circles. (b) The mixture of three types of superstructures, 20 nm × 20 nm, −0.9 V. The red, white, and blue unit cells correspond to the superstructure (11 × 8) R0°, (11 × 11) R0°, and (10 × 8) R10°.

is found that C_{60} molecules aggregate into a hexagonal structure, the same as C_{60} molecules in the local-order structure. However, the local-order structures, originating from the dim and bright molecules, turn into a long-range ordered ($\sqrt{93} \times \sqrt{93}$) R20° superstructure [Fig. 3(a)]. This superstructure is different from the structures of the C_{60} monolayer reported so far. There is a misorientation angle of 20° between the lattice directions of the C_{60} monolayer and the Bi(111) surface. The measured lattice constants of ($\sqrt{93} \times \sqrt{93}$) R20° are $b_1 = b_2 = 4.38 \pm 0.02$ nm, agreeing well with $\sqrt{93}$ times the lattice constant of Bi(111) (0.45 nm). Fig. 3(b) shows the schematic of the ($\sqrt{93} \times \sqrt{93}$) R20° superstructure. Based on the lattice constant of the Bi(111) substrate, the lattice vectors of the ($\sqrt{93} \times \sqrt{93}$) R20° superstructure can be expressed as following matrixes:

$$\begin{pmatrix} b_1 \\ b_2 \end{pmatrix} = \begin{pmatrix} 11 & -4 \\ 4 & 7 \end{pmatrix} \begin{pmatrix} a_1 \\ a_2 \end{pmatrix}$$

This ordered superstructure implies two things: first, the intermolecular interaction is getting stronger than that in the local-order structure prepared at low temperature (100 K). Second, the molecule–substrate interaction is also strong since the orientations of the C_{60} superstructure are commensurate with those of the substrate. Furthermore, we can clearly see that individual C_{60} molecules adopt various orientations, rather than the favorite orientations as C_{60} molecules in the local-order structure. As shown in the high-resolution STM image [Fig. 3(c)], C_{60} molecules in ($\sqrt{93} \times \sqrt{93}$) R20° present various shapes, such as two asymmetric lobes (white circle), two symmetrical lobes (yellow circle), and three lobes (blue circle),
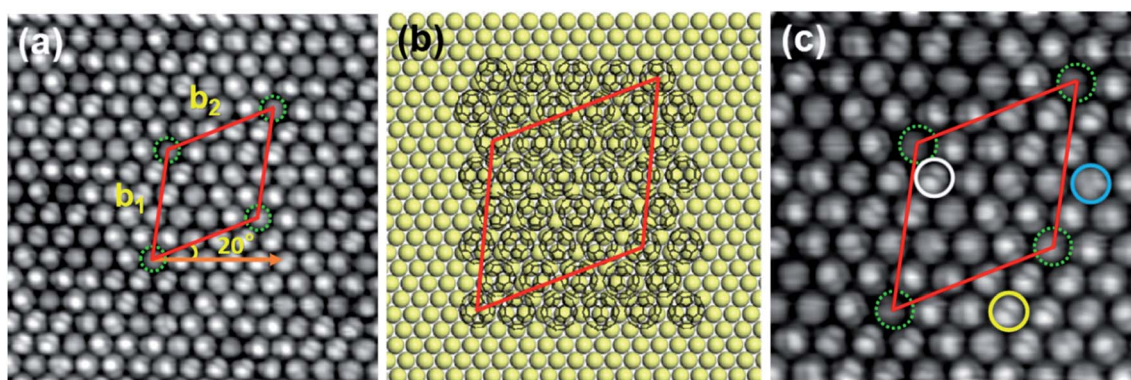

Fig. 3 (a) The STM image of the ($\sqrt{93} \times \sqrt{93}$) R20° superstructure, 15 nm × 15 nm, −1.2 V. (b) Schematic model of the ($\sqrt{93} \times \sqrt{93}$) R20° superstructure. The yellow balls and black hollow balls represent Bi atoms and C_{60} molecules. (c) High-resolution STM image of the ($\sqrt{93} \times \sqrt{93}$) R20° superstructure, 10 nm × 10 nm, −1.0 V. The individual molecules exhibit different orientations, such as 5 : 6 C−C bond, 6 : 6 C−C bond, and hexagon facing up, marked by white, yellow, and blue solid circles, respectively.
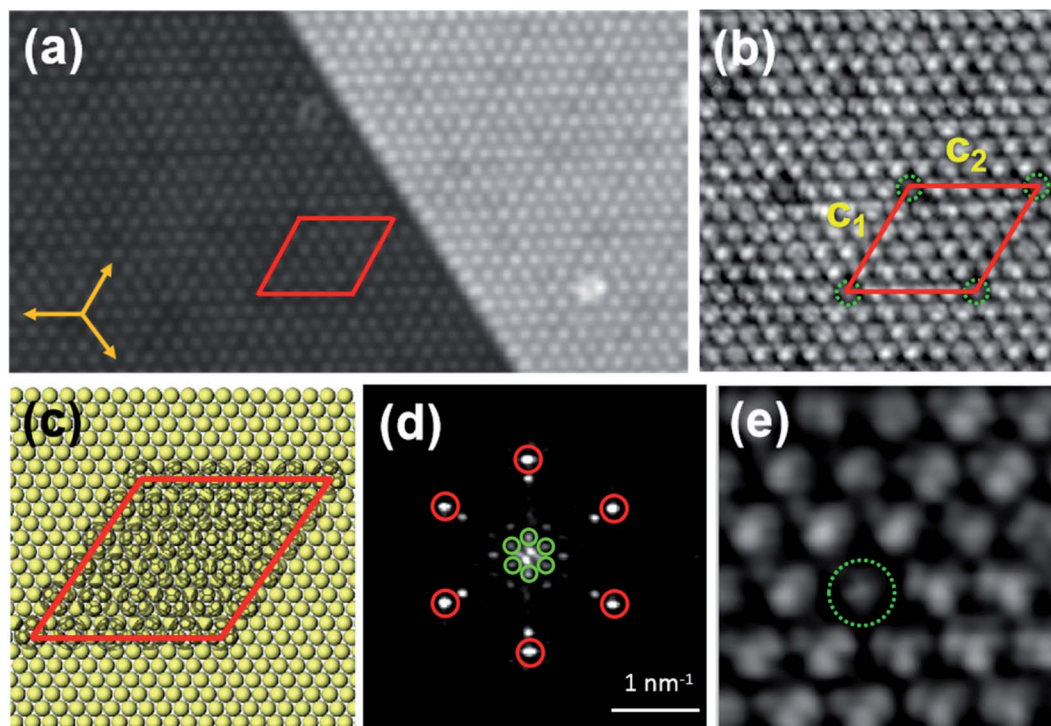
Fig. 4 (a) The STM image of the (11×11) R0° superstructure corresponding to the Bi(111), 39 nm × 21 nm, −1.5 V. (b) Close-up view of the (11×11) R0° superstructure, 14 nm × 14 nm, −0.7 V. (c) Schematic model of the (11×11) R0° superstructure with respect to the Bi(111) lattices. (d) FFT of the image (a). The spots marked by red circles correspond to the C_{60} hexagonal lattices, while the spots marked by the green circles represent the (11×11) R0° superstructure. (e) STM image with a sub-molecular resolution of the superstructure, 5 nm × 5 nm, −0.7 V.

corresponding to the $5:6$ C–C bond, $6:6$ C–C bond, and hexagon facing up. The diversity of C_{60} molecular orientations is due to the enhancement of intermolecular interaction in the $(\sqrt{93} \times \sqrt{93})$ R20° superstructure. The intermolecular interaction enables C_{60} molecules to overcome the molecule–substrate interaction and adopt other orientations, and then make the $(\sqrt{93} \times \sqrt{93})$ R20° superstructure stable.

When annealed at 400 K for about 20 min, C_{60} molecules still revealed a hexagonal lattice, while the superstructure transformed from $(\sqrt{93} \times \sqrt{93})$ R20° into (11×11) R0° superstructure [Fig. 4(a)], indicating that (11×11) R0° is more stable than $(\sqrt{93} \times \sqrt{93})$ R20°. The lattice directions of (11×11) R0° are along the directions of the Bi(111) substrate, and the lattice constants are $c_1 = c_2 = 5.00 \pm 0.02$ nm [Fig. 4(b)], corresponding to 11 times of the lattice constant of Bi(111). Fig. 4(d) is the fast Fourier transform (FFT) image of the (11×11) R0° superstructure, where the spots marked by red and green circles correspond to C_{60} hexagonal lattices and the (11×11) R0° superstructure. In the FFT image, the spots of the superstructure are clearly visible, though they are dimmer than the spots of C_{60} hexagonal lattices, implying that the (11×11) R0° superstructure has long-range order. The schematic model of (11×11) R0° is shown in Fig. 4(c). From STM images, the (11×11) R0° superstructure seems to have the same structure as the reported structure attributed to a Moiré pattern in ref. 36. However, in our experiment, the (11×11) R0° superstructure is transformed from the $(\sqrt{93} \times \sqrt{93})$ R20° superstructure and

have no relationship with the Moiré pattern. From the close-up view of the (11×11) R0° superstructure in Fig. 4(e), it is found that all the C_{60} molecules reveal a unified three-lobe structure, corresponding to the hexagon facing up, different from favorite orientations in the local-order structure and mixed orientations in $(\sqrt{93} \times \sqrt{93})$ R20°. With an increase in temperature, the superstructure of the C_{60} monolayer changes from local order to long-range order and C_{60} molecules are re-orientated. This is because the thermal diffusivities of C_{60} molecules and Bi atoms increase with the increase in temperature, which is conducive to the formation of a more orderly and stable superstructure.

Conclusions

In summary, the structure of C_{60} molecules on Bi(111) changes with temperature variation. When deposited on the Bi(111) surface at 100 K, C_{60} molecules form local-order structures, and the molecules in local-order structures adopt their favorite orientations. As the deposition temperature increases to room temperature, the local-order structures turn into a long-range ordered $(\sqrt{93} \times \sqrt{93})$ R20° superstructure. The orientations of C_{60} molecules in $(\sqrt{93} \times \sqrt{93})$ R20° superstructures are diverse. After annealing at 400 K for about 20 min, the C_{60} film exhibits a (11×11) R0° superstructure, and all C_{60} molecules in this superstructure take the unified orientation, hexagon facing-up. The appearance of numerous superstructures and the molecular orientations in superstructures is due to the change in the

thermal diffusivity of C_{60} molecules and Bi atoms at different temperatures.

Conflicts of interest

There are no conflicts to declare.

Acknowledgements

References

1 T. Ohtsuki, K. Masumoto, K. Ohno, Y. Maruyma, Y. Kawazoe, K. Sueki and K. Kikuchi, Insertion of Be Atoms in C_{60} Fullerene Cages: Be@C_{60}, *Phys. Rev. Lett.*, 1996, **77**, 3522.

2 C. Deibel and V. Dyakonov, Polymer–fullerene bulk heterojunction solar cells, *Rep. Prog. Phys.*, 2010, **73**, 096401.

3 D. J. Hornbaker, S.-J. Kahng, S. Misra, B. W. Smith, A. T. Johnson, E. J. Mele, D. E. Luzzi and A. Yazdani, Mapping the One-Dimensional Electronic States of Nanotube Peapod Structures, *Science*, 2002, **295**, 828–831.

4 H. Park, J. Park, A. K. L. Lim, E. H. Anderson, A. P. Alivisatos and P. L. McEuen, Nanomechanical oscillations in a single-C_{60} transistor, *Nature*, 2000, **407**, 57–60.

5 P. W. Stephens, G. Bortel, G. Faigel, M. Tegze, A. Jánossy, S. Pekker, G. Oszlanyi and L. Forró, Polymeric fullerene chains in RbC$_{60}$ and KC$_{60}$, *Nature*, 1994, **370**, 636–639.

6 R. Yamachika, M. Grobis, A. Wachowiak and M. F. Crommie, Controlled atomic doping of a single molecule, *Science*, 2004, **304**, 281–284.

7 H. I. Li, K. Pussi, K. J. Hanna, L. L. Wang, D. D. Johnson, H. P. Cheng, H. Shin, S. Curtarolo, W. Moritz and J. A. Smerdon, Surface Geometry of C_{60} on Ag(111), *Phys. Rev. Lett.*, 2009, **103**, 056101.

8 K. Pussi, H. I. Li, H. Shin, L. N. S. Loli, A. K. Shukla, J. Ledieu, V. Fournee, L. L. Wang, S. Y. Su and K. E. Marino, Elucidating the dynamical equilibrium of C_{60} molecules on Ag(111), *Phys. Rev. B: Condens. Matter Mater. Phys.*, 2012, **86**, 205426.

9 H. I. Li, G. J. P. Abreu, A. K. Shukla, V. Fournée, J. Ledieu, L. N. Serkovic Loli, S. E. Rauterkus, M. V. Snyder, S. Y. Su and K. E. Marino, Ordering and dynamical properties of superbright C_{60} molecules on Ag(111), *Phys. Rev. B: Condens. Matter Mater. Phys.*, 2014, **89**, 085428.

10 L. Tang, Y. Xie and Q. Guo, Complex orientational ordering of C_{60} molecules on Au(111), *J. Chem. Phys.*, 2011, **135**, 11470211.

11 X. Torrelles, M. Pedio, C. Cepek and R. Felici, $(2\sqrt{3} \times 2\sqrt{3})$ R30 degrees induced self-assembly ordering by C_{60} on a Au(111) surface: X-ray diffraction structure analysis, *Phys. Rev. B: Condens. Matter Mater. Phys.*, 2012, **86**, 075461.

12 M. Passens, R. Waser and S. Karthaeuser, Enhanced fullerene-Au(111) coupling in $(2\sqrt{3} \times 2\sqrt{3})$R30 degrees superstructures with intermolecular interactions, *Beilstein J. Nanotechnol.*, 2015, **6**, 1421–1431.

13 H. Shin, A. Schwarze, R. D. Diehl, K. Pussi, A. Colombier, E. Gaudry, J. Ledieu, G. M. McGuirk, L. N. S. Loli and V. Fournee, Structure and dynamics of C_{60} molecules on Au(111), *Phys. Rev. B: Condens. Matter Mater. Phys.*, 2014, **89**, 245428.

14 G. Schull and R. Berndt, Orientationally ordered (7×7) superstructure of C_{60} on Au(111), *Phys. Rev. Lett.*, 2007, **99**, 226105.

15 X. Zhang, F. Yin, R. E. Palmer and Q. Guo, The C_{60}/Au(111) interface at room temperature: A scanning tunnelling microscopy study, *Surf. Sci.*, 2008, **602**, 885–892.

16 J. A. Gardener, G. A. D. Briggs and M. R. Castell, Scanning tunneling microscopy studies of C_{60} monolayers on Au(111), *Phys. Rev. B: Condens. Matter Mater. Phys.*, 2009, **80**, 235434.

17 Y. Z. Shang, Z. L. Wang, D. X. Yang, Y. Y. Wang, C. K. Ma, M. L. Tao, K. Sun, J. Y. Yang and J. Z. Wang, Orientation ordering and chiral superstructures in fullerene monolayer on Cd(0001), *Nanomaterials*, 2020, **10**, 1305.

18 S. Han, M. X. Guan, C. L. Song, Y. L. Wang, M. Q. Ren, S. Meng, X. C. Ma and Q. K. Xue, Visualizing molecular orientational ordering and electronic structure in CsnC$_{60}$ fulleride films, *Phys. Rev. B*, 2020, **101**, 085413.

19 W. W. Pai and C. L. Hsu, Ordering of an incommensurate molecular layer with adsorbate-induced reconstruction:C_{60}/Ag(100), *Phys. Rev. B: Condens. Matter Mater. Phys.*, 2003, **68**, 121403.

20 C. Grosse, O. Gunnarsson, P. Merino, K. Kuhnke and K. Kern, Nanoscale Imaging of Charge Carrier and Exciton Trapping at Structural Defects in Organic Semiconductors, *Nano Lett.*, 2016, **16**, 2084–2089.

21 L. Tang, X. Zhang, Q. Guo, Y. Wu, L. Wang and H. Cheng, Two bonding configurations for individually adsorbed C_{60} molecules on Au(111), *Phys. Rev. B: Condens. Matter Mater. Phys.*, 2010, **82**, 125414.

22 L. Tang, X. Zhang and Q. Guo, Organizing C_{60} molecules on a nanostructured Au(111) surface, *Surf. Sci.*, 2010, **604**, 1310–1314.

23 T. Hashizume, K. Motai, X. D. Wang, H. Shinohara, Y. Saito, Y. Maruyama, K. Ohno, Y. Kawazoe, Y. Nishina and H. W. Pickering, Intramolecular structures of C_{60} molecules adsorbed on the Cu(111)-(1×1) surface, *Phys. Rev. Lett.*, 1993, **71**, 2959–2962.

24 S. Wong, W. W. Pai, C. Chen and M. Lin, Coverage-dependent adsorption superstructure transition of C_{60}/Cu(001), *Phys. Rev. B: Condens. Matter Mater. Phys.*, 2010, **82**, 125442.

25 G. Xu, X. Shi, R. Q. Zhang, W. W. Pai, H. T. Jeng and M. A. Van Hove, Detailed low-energy electron diffraction analysis of the (4×4) surface structure of C_{60} on Cu(111): Seven-atom-vacancy reconstruction, *Phys. Rev. B: Condens. Matter Mater. Phys.*, 2012, **86**, 075419.

26 G. Li, H. T. Zhou, L. D. Pan, Y. Zhang, J. H. Mao, Q. Zou, H. M. Guo, Y. L. Wang, S. X. Du and H. J. Gao, Self-assembly of C_{60} monolayer on epitaxially grown, nanostructured graphene on Ru(0001) surface, *Appl. Phys. Lett.*, 2012, **100**, 0133041.

27 M. Jung, D. Shin, S. Sohn, S. Kwon, N. Park and H. Shin, Atomically resolved orientational ordering of C_{60} molecules on epitaxial graphene on Cu(111), *Nanoscale*, 2014, **6**, 11835–11840.

28 J. G. Hou, J. L. Yang, H. Q. Wang, Q. X. Li, C. G. Zeng, H. Lin, W. Bing, D. M. Chen and Q. S. Zhu, Identifying molecular orientation of individual C_{60} on a Si(111)-(7 × 7) surface, *Phys. Rev. Lett.*, 1999, **83**, 3001–3004.

29 H. Q. Wang, C. G. Zeng, B. Wang, J. G. Hou, Q. X. Li and J. L. Yang, Orientational configurations of the C_{60} molecules in the (2 × 2) superlattice on a solid C_{60} (111) surface at low temperature, *Phys. Rev. B: Condens. Matter Mater. Phys.*, 2001, **63**, 085417.

30 A. Goldoni, C. Cepek, M. De Seta, J. Avila, M. C. Asensio and M. Sancrotti, Interaction of C_{60} with Ge(111) in the $3\sqrt{3} \times 3\sqrt{3}$ R30° phase: A (2 × 2) model, *Phys. Rev. B: Condens. Matter Mater. Phys.*, 2000, **61**, 10411–10416.

31 J. Leaf, A. Stannard, S. P. Jarvis, P. Moriarty and J. L. Dunn, A combined monte carlo and huckel theory simulation of orientational ordering in C_{60} assemblies, *J. Phys. Chem. C*, 2016, **120**, 8139–8147.

32 G. E. Thayer, J. T. Sadowski, F. M. z. Heringdorf, T. Sakurai and R. M. Tromp, Role of surface electronic structure in thin film molecular ordering, *Phys. Rev. Lett.*, 2005, **95**, 25610.

33 K. Sun, M. Lan and J. Z. Wang, Absolute configuration and chiral self-assembly of rubrene on Bi(111), *Phys. Chem. Chem. Phys.*, 2015, **17**, 26220.

34 M. L. Tao, Y. B. Tu, K. Sun, Y. Zhang, X. Zhang, Z. B. Li, S. J. Hao, H. F. Xiao, J. Ye and J. Z. Wang, Structural transitions in different monolayers of cobalt phthalocyanine film grown on Bi(111), *J. Phys. D: Appl. Phys.*, 2016, **49**, 015307.

35 J. T. Sadowski, R. Z. Bakhtizin, A. I. Oreshkin, T. Nishihara, A. Al-Mahboob, Y. Fujikawa, K. Nakajima and T. Sakurai, Epitaxial C_{60} thin films on Bi(0001), *Surf. Sci.*, 2007, **601**, 136–139.

36 T. Nagao, J. T. Sadowski, M. Saito, S. Yaginuma, Y. Fujikawa, T. Kogure, T. Ohno, Y. Hasegawa, S. Hasegawa and T. Sakurai, Nanofilm allotrope and phase transformation of ultrathin Bi film on Si(111)−7 × 7, *Phys. Rev. Lett.*, 2004, **93**, 105501.

37 X. Q. Shi, A. M. Van Hove and R. Q. Zhang, Survey of structural and electronic properties of C_{60} on close-packed metal surfaces, *J. Mater. Sci.*, 2012, **47**, 7341–7355.

38 W. W. Pai, H. T. Jeng, C. M. Cheng, C. H. Lin, X. Xiao, A. Zhao, X. Zhang, G. Xu, X. Q. Shi, M. A. Van Hove, C. S. Hsue and K. D. Tsuei, Optimal electron doping of a C_{60} monolayer on Cu(111) via interface reconstruction, *Phys. Rev. Lett.*, 2010, **104**, 036103.